Giant Clusters with Unusual Electronic and Magnetic Structures Due to Open Shell Metal Centers Embedded Far Apart from Each Other: Spin Frustration and Antisymmetric Exchange

Dante Gatteschi,*,† Roberta Sessoli,† Winfried Plass,‡ Achim Müller,*,‡ Erich Krickemeyer,‡ Jochen Meyer,‡ Dirk Sölter,‡ and Peter Adler§

Dipartimento di Chimica, Università di Firenze, I-50144 Firenze, Italy, Fakultät für Chemie, Lehrstuhl für Anorganische Chemie I, Universität Bielefeld, D-33501 Bielefeld, Germany, and Max-Planck-Institut für Festkörperforschung, D-70569 Stuttgart, Germany

Received August 18, 1995[⊗]

The magnetic properties of the compounds $(NH_4)_{21}[\{VO(H_2O)\}_6\{Mo(\mu\text{-}H_2O)_2(\mu\text{-}OH)Mo\}_3\{Mo_{15}(MoNO)_2O_{58}(H_2O)_2\}_3]\cdot 65H_2O$, **1a**, $(NH_2Me_2)_{18}(NH_4)_6[\{VO(H_2O)\}_6\{Mo(\mu\text{-}H_2O)_2(\mu\text{-}O)Mo\}_3\{Mo_{15}(MoNO)_2O_{58}(H_2O)_2\}_3]\cdot 14H_2O$, **1b**, and $Na_3(NH_4)_{12}[\{Fe(H_2O)_2\}_6\{Mo(\mu\text{-}H_2O)_2(\mu\text{-}OH)Mo\}_3\{Mo_{15}(MoNO)_2O_{58}(H_2O)_2\}_3]\cdot 76H_2O$, **2**, have been investigated. **1a**, **1b**, and **2** contain giant cluster anions composed of three transferable Mo_{17} ligands bridged by cationic centers which can be exchanged for other metal centers (this means that metal centers can be placed deliberately on the surface of large clusters serving as models for metal oxides). Six of these paramagnetic centers (V(IV) in **1a**/**1b** and Fe(III) in **2**) are arranged to form a trigonal prism. The analysis of the magnetic susceptibility data reveals an efficient exchange pathway between the centers located within the trigonal face of this prism mediated by the large and electronically unusual Mo_{17} ligands. In the case of the vanadium(IV) compounds a remarkably strong antiferromagnetic coupling within the triangles (V···V distances > 650 pm) is observed, ca. 190 cm^{-1} for **1a** and ca. 160 cm^{-1} for **1b**, with the Hamiltonian defined as $\hat{H} = J\sum_{i<j}\mathbf{S}_i\cdot\mathbf{S}_j$. The measurement of the anisotropic susceptibility of compound **1a** allowed us to determine for the first time the elusive antisymmetric exchange parameter *G*, expected to be generally operative in spin frustrated systems. The electronic structure of the giant cluster anions of **1a**, **1b**, and **2** as well as, for the purpose of comparison, those of the compounds $(NH_4)_{12}[\{MoO_2\}_2\{H_{12}Mo_{15}(MoNO)_2O_{58}(H_2O)_2\}_2]\cdot 33H_2O$, **3**, $Na_8[\{MoO_2\}_2\{H_{12}Mo_{15}(MoO)_2O_{58}(H_2O)_2\}_2]\cdot 58H_2O$, **4**, and $(NH_2Me_2)_6[H_2H_{12}(Mo^{VI}O_3)_4Mo^{V}{}_{12}O_{40}]$, **5**, have been investigated by photoelectron spectroscopy and extended Hückel calculations.

Introduction

The magnetic properties of large spin clusters, which eventually can give rise to magnetic nanoclusters, i.e. magnetic particles of nanometer dimensions, are attracting increasing interest.[1] There are several good reasons for this, ranging from attempts to validate quantum theory to design new magnetic refrigerators, over developing models for biomineralization and the functioning of ferritin to determining the nature of interstellar aggregates.[2]

There are several different chemical approaches for the synthesis of magnetic nanoclusters. It is possible to embed the particles in protecting media, like proteinic shells or micelles, polymers, or resins, but in this case it is difficult to achieve monodispersed and easily characterized particles. Perhaps the most challenging approach is that of making giant molecular species which can be characterized with the usual approaches of molecular chemistry. This route has previously been followed for high nuclearity metal clusters,[3] and now suitable methods are being followed for obtaining similar results with transition metal oxo clusters.[4] All the synthetic strategies must design ingenious methods of avoiding the growth of the particles, which otherwise would form the bulk metal oxides or hydroxides, of large dimensions. It is therefore necessary that at some stage the growth of the developing particles is blocked by the presence of unreactive groups on the periphery of the particles themselves. This can be achieved either with the presence of suitable ligands or with the formation of M═O bonds with low nucleophilicity. The latter approach has long been known, since it is the basis of the formation of the well-known polyoxometalates.[5] For a long time this was limited to d^0 ions, which do not form giant species and are not

† University of Florence.
‡ University of Bielefeld.
§ Max-Planck-Institut, Stuttgart.
⊗ Abstract published in *Advance ACS Abstracts,* March 1, 1996.

(1) (a) Gatteschi, D.; Caneschi, A.; Pardi, L.; Sessoli, R. *Science* **1994**, *265*, 1054. (b) Gatteschi, D. *Adv. Mater*. **1994**, *6*, 635. (c) Jena, P. *Physics and Chemistry of Finite Systems: From Clusters to Metals*; Kluwer Academic Publishers: Dordrecht, The Netherlands, 1992.

(2) (a) Leggett, A. J. *J. Phys. Rev. B* **1984**, *30*, 1208. (b) Awschalom, D. D.; DiVincenzo, D. P.; Smyth, J. F. *Science* **1992**, *258*, 414. (c) Balcells, L.; Tholence, J. L.; Linderoth, S.; Barbara, B.; Tejada, J. *Z. Phys. B* **1992**, *89*, 209. (d) Barbara, B.; Sampaio, L. C.; Wegrowe, J. E.; Ratnam, B. A.; Marchand, A.; Paulsen, C.; Novak, M. A.; Tholence, J. L.; Uehara, M.; Fruchart, D. *J. Appl. Phys*. **1993**, *73*, 6703. (e) Mann, S.; Frankel, R. B. In *Biomineralization—Chemical and Biochemical Perspectives*; Mann, S., Webb, J., Williams, R. J. P., Eds.; VCH: Weinheim, Germany, 1989; p 389. (f) Meldrum, F. C.; Heywood, B. R.; Mann, S. *Science* **1992**, *257*, 522. (g) Ziolo, R. F.; Giannelis, E. P.; Weinstein, B. A.; O'Horo, M. P.; Ganguly, B. N.; Mehrotra, V.; Russell, M. W.; Huffman, D. R. *Science* **1992**, *257*, 219.

(3) Schmid, G.; Klein, N. *Angew. Chem., Int. Ed. Engl*. **1986**, *25*, 910.

(4) (a) Taft, K. L.; Lippard, S. J. *J. Am. Chem. Soc*. **1990**, *112*, 9629. (b) Schake, A. R.; Vincent, J. B.; Li, Q.; Boyd, P. D. W.; Folting, K.; Huffman, J. C.; Hendrickson, D. N.; Christou, G. *Inorg. Chem*. **1989**, *28*, 1915. (c) Goldberg, D. P.; Caneschi, A.; Lippard, S. J. *J. Am. Chem. Soc*. **1993**, *115*, 9299. (d) Lippard, S. J. *Angew. Chem., Int. Ed. Engl*. **1988**, *27*, 344. (e) Heath, S. L.; Powell, A. K. *Angew. Chem., Int. Ed. Engl*. **1992**, *31*, 191. (f) Taft, K. L.; Papaefthymiou, G. C.; Lippard, S. J. *Science* **1993**, *259*, 1302.

(5) (a) Pope, M. T.; Müller, A. *Angew. Chem., Int. Ed. Engl*. **1991**, *30*, 34. (b) Pope, M. T.; Müller, A., Eds. *Polyoxometalates: From Platonic Solids to Anti-Retroviral Activity*; Kluwer Academic Publishers: Dordrecht, The Netherlands, 1994.

0020-1669/96/1335-1926$12.00/0

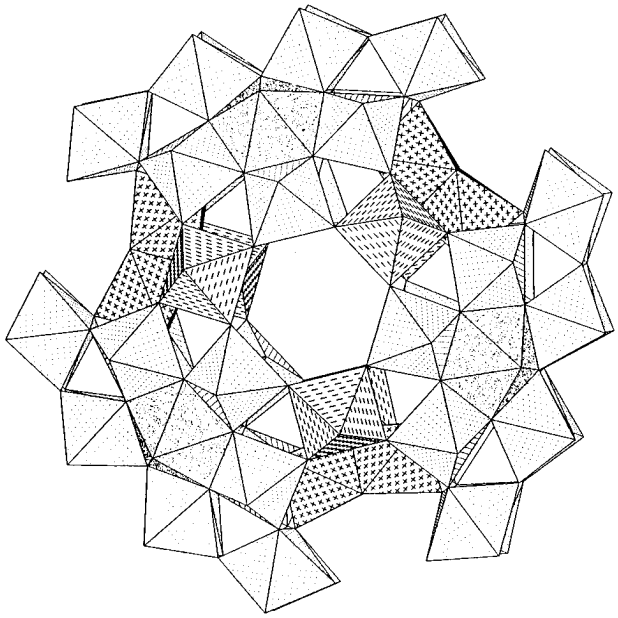

Figure 1. Polyhedral representation of the cluster anions of **1a** (**1b**) and **2**. The $OVO_4(OH_2)$ octahedra in **1a** (**1b**) and the $FeO_4(OH_2)_2$ octahedra in **2**, respectively, are shown with broken lines, the $\{Mo(\mu\text{-}H_2O)_2(\mu\text{-}OH)Mo\}$ moieties with crosses, the pentagonal $Mo(NO)O_6$ bipyramids are randomly dotted, and the MoO_6 octahedra have a regular pattern of dots; the view is approximately along the $\bar{6}$ (S_3) axis.

interesting from the magnetic point of view, but recently new classes of polyoxometalates containing magnetic centers mainly oxovanadium(IV) ions have been reported.

In this context some of us showed how polyoxometalates can be used also in a different way to produce large spin clusters.[6] By using large quasi-preorganized building blocks of polyoxometalates as ligands toward magnetic metal centers, it was possible to obtain giant clusters of the following formulas:[6,7]

$$(NH_4)_{21}[\{VO(H_2O)\}_6\{Mo(\mu\text{-}H_2O)_2(\mu\text{-}OH)Mo\}_3\{Mo_{15}(MoNO)_2O_{58}(H_2O)_2\}_3]\cdot 65H_2O \quad \textbf{(1a)}$$

$$(NH_2Me_2)_{18}(NH_4)_6[\{VO(H_2O)\}_6\{Mo(\mu\text{-}H_2O)_2(\mu\text{-}O)Mo\}_3\{Mo_{15}(MoNO)_2O_{58}(H_2O)_2\}_3]\cdot 14H_2O \quad \textbf{(1b)}$$

$$Na_3(NH_4)_{12}[\{Fe(H_2O)_2\}_6\{Mo(\mu\text{-}H_2O)_2(\mu\text{-}OH)Mo\}_3\{Mo_{15}(MoNO)_2O_{58}(H_2O)_2\}_3]\cdot 76H_2O \quad \textbf{(2)}$$

In these clusters with molecular masses of the anion larger than 9 kDa, that means of the order of small proteins, the six metal centers (oxovanadium(IV) or iron(III)) and three formally cationic $\{Mo(\mu\text{-}H_2O)_2(\mu\text{-}OH)Mo\}^{9+}$ moieties (in the case of **1b**, the μ-OH groups are deprotonated) connect three Mo_{17} ligands, $\{Mo^{VI}{}_{15}(MoNO)^{3+}{}_2O_{58}(H_2O)_2\}^{20-}$, as shown in Figure 1. The molybdenum(VI)-based polyoxometalates act as embedding agents for the "active site", containing six oxovanadium(IV) and six iron(III) centers, respectively (see Figure 1). The formulation of the structure is based on the following investigations: single-crystal X-ray diffraction studies as well as IR/Raman, UV/vis/near-IR, ESR spectroscopy, XPS, redox titrations with MnO_4^-, bond valence sum calculations, elemental analyses, and thermogravimetric studies.[6,7]

It is tempting to describe these clusters formally as inorganic equivalents of small proteins, in which the molybdenum moieties have a structural function, providing the shape of the cluster and leaving the space available for the magnetically active sites. However, they may also have a more important role, by *transmitting the magnetic interaction between the "active centers"*. In order to clarify the relative roles of the various moieties we investigated in detail the magnetic properties of **1a**, **1b**, and **2**, performing also photoelectron spectroscopy and extended Hückel MO calculations in order to elucidate the electronic structure of these giant cluster anions.

Experimental Section

The compounds $(NH_4)_{21}[Mo_{57}(VO)_6(NO)_6O_{174}(OH)_3(H_2O)_{18}]\cdot 65H_2O$,[7] **1a**, $(NH_2Me_2)_{18}(NH_4)_6[Mo_{57}(VO)_6(NO)_6O_{177}(H_2O)_{18}]\cdot 14H_2O$,[7] **1b**, $Na_3(NH_4)_{12}[Mo_{57}Fe_6(NO)_6O_{174}(OH)_3(H_2O)_{24}]\cdot 76H_2O$,[6] **2**, $(NH_4)_{12}[Mo_{36}(NO)_4O_{108}(H_2O)_{16}]\cdot 33H_2O$,[7] **3**, $Na_8[Mo_{36}O_{112}(H_2O)_{16}]\cdot 58H_2O$,[8] **4**, and $(NH_2Me_2)_6[H_2Mo_{16}(OH)_{12}O_{40}]$,[9] **5**, have been prepared as previously described. Microcrystalline samples were satisfactorily analyzed.

Photoelectron Spectroscopy. Photoelectron spectra of **1b**, **2**, **3**, **4**, and **5** were measured with a Leybold-Heraeus LHS-10 spectrometer with Mg Kα radiation for the core level as well as Al Kα and He II radiation for the valence band spectra. The radiation of the excitation sources was nonmonochromatic, and the electron pass energies were 50 eV for XP and 10 eV for UP spectra. In addition, valence band and Mo 4p spectra of a molybdenum foil, the surface of which was cleaned by argon ion sputtering, were measured for purposes of comparison. Since the cluster compounds are insulators, surface charging of several electron-volts occurred. A charging correction for the XP spectra was estimated from the surface carbon contamination C 1s peak, the binding energy of which was set to $E_B = 285$ eV. This leads to binding energies of 286.5 and 286.8 eV for the intrinsic C 1s peaks arising from the $(H_2NMe_2)^+$ cations in **1b** and **5**, respectively. The difference 0.3 eV gives an estimate for the error in binding energies associated with the calibration procedure. The crystal water of the compounds evaporates under UHV conditions. During the measurements the samples were cooled with liquid nitrogen. For collecting He II spectra the samples were flooded with low energy electrons. In order to facilitate comparison of XP and UP valence band spectra the UP spectra were shifted so that the top of the valence bands of XP and UP spectra coincided.

Magnetochemistry. The magnetic susceptibility was measured using a Metronique Ingenierie SQUID Magnetometer with an applied field of 10 kOe. The low temperature data of **2** were collected with $H = 1$ kOe to avoid saturation effects. The experimental data were corrected for diamagnetic contributions and temperature-independent paramagnetism based on the results obtained for compound **3** (see Results and Discussion). The magnetic anisotropy of **1b** was determined by gluing about 20 crystals (ca. 100 mg) on a thin glass support with the 001 face parallel to the support. The susceptibility was then measured with the field applied parallel and perpendicular to the unique *c* axis. As the compound crystallizes in a hexagonal ($P6_3/mmc$) space group, only these two directions are required to determine the magnetic anisotropy.

Results and Discussion

Structures. The structures of **1a**, **1b**, and **2**, the cluster anions of which have D_{3h} symmetry, have been previously reported[6,7] and briefly described in the Introduction. The most interesting feature, and a very delicate one for the description of the magnetic properties, is that at least three different types of molybdenum centers are present in these giant clusters. Structural evidence suggests that the cationic fragments $\{Mo(\mu\text{-}H_2O)_2(\mu\text{-}OH)Mo\}^{9+}$ contain formally molybdenum(V) centers. On the other hand the fragments $\{Mo^{VI}{}_{15}(MoNO)^{3+}{}_2O_{58}$-

(6) Müller, A.; Plass, W.; Krickemeyer, E.; Dillinger, S.; Bögge, H.; Armatage, A.; Proust, A.; Beugholt, C.; Bergmann, U. *Angew. Chem., Int. Ed. Engl.* **1994**, *33*, 849.
(7) Müller, A.; Krickemeyer, E.; Dillinger, S.; Bögge, H.; Plass, W.; Proust, A.; Dloczik, L.; Menke, C.; Meyer, J.; Rohlfing, R. *Z. Anorg. Allg. Chem.* **1994**, *620*, 599.
(8) Krebs, B.; Stiller, S.; Tytko, K. H.; Mehmke, J. *Eur. J. Solid State Inorg. Chem.* **1991**, *28*, 883.
(9) Kahn, M. I.; Müller, A.; Dillinger, S.; Bögge, H.; Chen, Q.; Zubieta, J. *Angew. Chem., Int. Ed. Engl.* **1993**, *32*, 1780.

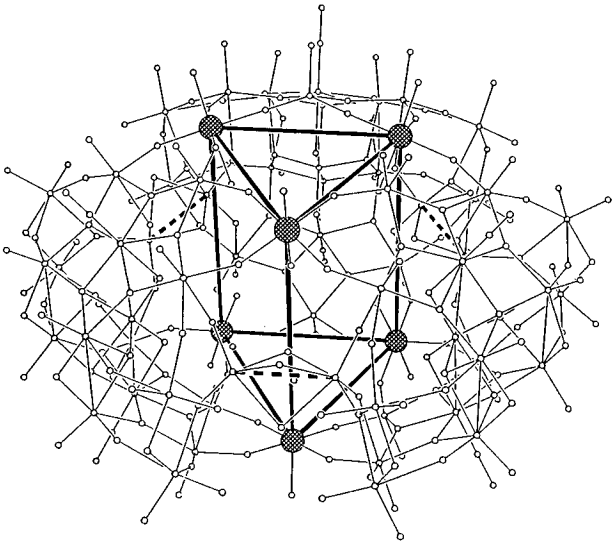

Figure 2. Ball-and-stick model of the cluster anions of **1a** (**1b**) and **2** with an illustration of the trigonal prism formed by the paramagnetic metal centers **M** (for metal−metal distances see text). The position of the three {Mo(μ-H_2O)$_2$(μ-OH)Mo} pairs on the horizontal mirror plane is indicated by broken lines.

$(H_2O)_2\}^{20-}$, which are also present in $(NH_4)_{12}[\{MoO_2\}_2\{H_{12}Mo_{15}(MoNO)_2O_{58}(H_2O)_2\}_2]\cdot 33H_2O$, **3**, contain only diamagnetic centers (molybdenum(VI) centers and $(MoNO)^{3+}$ units). However, since the accurate description of the valences on the various metal centers is of paramount importance for the understanding of the magnetic properties, we performed photoelectron spectroscopy measurements, the results of which are described below.

The six magnetic centers **M**, oxovanadium(IV) in **1a** and **1b** and iron(III) in **2**, are assembled in two layers of three. These define a trigonal prism with metal−metal distances of 655.9 (**1a**), 654.3 (**1b**), and 640.2 pm (**2**) in the triangular faces, and 960.2 (**1a**), 958.7 (**1b**), and 897.4 pm (**2**) in the vertical rectangular faces (see Figure 2). The trigonal prism is linked by the three transferable Mo_{17} ligands located above the three rectangular faces. Along the edges of the trigonal faces the **M** centers are connected by O−Mo(VI)−O bridges, therefore forming two **M**−O−Mo−O 12-membered rings (**M** = Fe and V). The connection of **M** centers belonging to different triangles occurs through a seven atom O−Mo(VI)−O−Mo(V)−O−Mo(VI)−O bridge (cf. Figures 1 and 2).

Photoelectron Spectroscopy. Photoelectron spectra have been measured for **1b**, **2**, and **3** in order to understand their unusual electronic properties. Since it is in general difficult to separate the contributions to the photoelectron spectra arising from the different kinds of metal sites we also investigated the cluster compounds $Na_8[\{MoO_2\}_2\{H_{12}Mo_{15}(MoO)_2O_{58}(H_2O)_2\}_2]\cdot 58H_2O$, **4**, where only Mo(VI) sites are present, as well as $(NH_2Me_2)_6[H_2H_{12}(Mo^{VI}O_3)_4Mo^{V}{}_{12}O_{40}]$, **5**, where the major part of the molybdenum atoms are in the +5 oxidation state.

The spectra show for the O 1s core level signals either a broadened single line (**3** and **5**) or a double peak structure with a main component and a sidepeak with less intensity at higher binding energy (**1b**, **2**, and **4**). The E_B values which correspond to the main components range from 530.8 to 531.6 eV as observed in other oxomolybdates.[10] The sidepeak observed at about 2 eV higher binding energy arises presumably from surface-adsorbed water molecules and/or from other surface contaminations.

(10) Patterson, T. A.; Carver, J. C.; Leyden, D. E.; Hercules, D. M. *J. Phys. Chem.* **1976**, *80*, 1700.

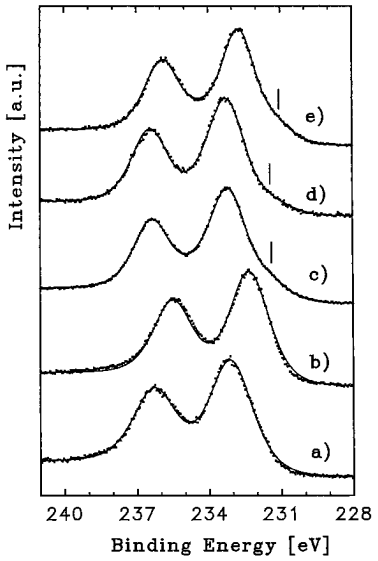

Figure 3. Representation of the Mo 3d core level signals in the XP spectra of (a) **4**, (b) **5**, (c) **3**, (d) **1b**, and (e) **2**. Solid curves correspond to the best fits with one line for each spin-orbit component in cases a and b, and two lines in cases c−e. In the latter cases, a vertical bar indicates the position of the shoulder corresponding to a component with lower binding energy.

Information about the oxidation states of the molybdenum atoms can be derived from the Mo 3d core level signals, which are composed of the $3d_{5/2}$ spin−orbit components at lower and the $3d_{3/2}$ ones at higher binding energies. In the case of **4** and **5** (Figure 3a,b) each spin−orbit component consists mainly of one line with peak maxima at 233.0 and 232.3 eV, respectively. In agreement with the expectation of an increasing binding energy with increasing oxidation number, which is indeed observed in other oxomolybdates,[10,11] E_B is found to be larger for **4** than for **5**. The resolution of the XP spectra is, however, too small to resolve the peaks due to the molybdenum(V) and molybdenum(VI) sites in **5**.

The Mo $3d_{5/2}$ signals of **1b**, **2**, and **3** (Figure 3c−e) reveal a main line at about 233.0 (±0.3) eV. The high binding energies are typical for molybdenum(VI) centers, which is indeed the oxidation state of most of the molybdenum atoms in the clusters. In addition, a weak feature at ca. 1.7 eV lower binding energy occurs.[12] An unambiguous interpretation of the spectra is complicated by the fact that after prolonged irradiation with X-rays the spectra broaden toward the low binding energy side which corresponds to the progressive reduction of molybdenum(VI) to molybdenum(V) under UHV conditions. The E_B value corresponding to this nonintrinsic molybdenum(V) component is only 1.2 eV smaller in binding energy than that corresponding to the main component. Therefore, the shoulder at low binding energy seen already in the spectra soon after the beginning of the measurements is considered as intrinsic and attributed to the molybdenum atoms from the $(MoNO)^{3+}$ groups. This assignment is supported by comparison of the Mo 3d signals of **3** and **4**. The $3d_{5/2}$ line of **4** does not reveal the low binding energy shoulder seen in the spectrum of **3**.

For **1b** and **2** six molybdenum(V) sites arising essentially from the {Mo(μ-H_2O)$_2$(μ-OH)Mo}$^{9+}$ moieties are present in

(11) Wagner, C. D., Riggs, W. M., Davis, L. E., Moulder, J. F., Muilenberg, G. E., Eds. *Handbook of X-Ray Photoelectron Spectroscopy*; Perkin-Elmer Corporation: 1978.

(12) For a quantitative analysis the Mo 3d spectra were fitted to lines of mixed Lorentzian−Gaussian line shapes. The intensity ratios $I(3d_{5/2})/I(3d_{3/2})$ were fixed at the theoretical value of 1.5, and the known spin−orbit splitting of 3.2 eV was used.

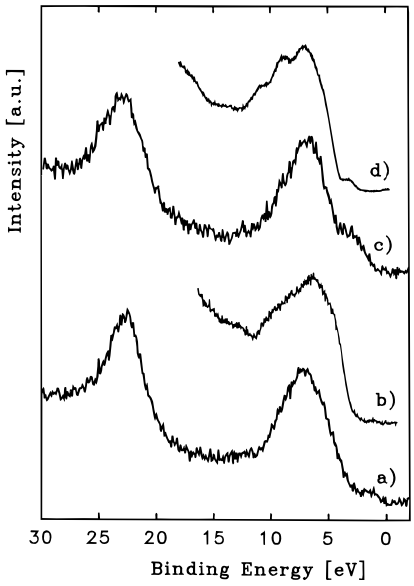

Figure 4. Valence band region of the photoelectron spectra of **4** (bottom, a and b) and **5** (top, c and d) excited with nonmonochromatic Al Kα radiation (a and c) and He II radiation (b and d). In the XP spectra also the band at 23 eV corresponding to the O 2s levels is included.

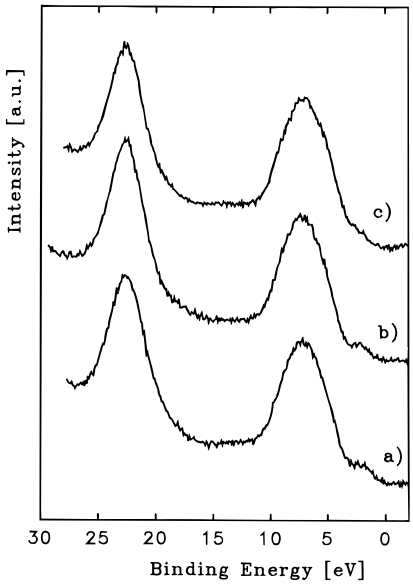

Figure 5. Valence band region of the photoelectron spectra (Al Kα radiation) of (a) **3**, (b) **1b**, and (c) **2**. For easier comparison the spectra have been aligned to equal O 2s binding energies.

addition to the 45 molybdenum(VI) and six Mo centers from the $(MoNO)^{3+}$ groups. The binding energy difference between molybdenum(V) and molybdenum(VI) sites again is not large enough to allow the resolution of such a small molybdenum-(V) fraction in the present XP spectra.

For describing the essential features of the electronic structure of the compounds we should refer to the valence band spectra of **4** and **5** (Figure 4). For **4** the Al Kα spectrum basically consists of a broad band with a width at half height of 4.5 eV. The integrated intensity for the valence band features is even larger than the corresponding O 2s intensity (ratio: 1.17). On the other hand, from the atomic photoionization cross sections,[13] it is expected that the partial intensity corresponding to O 2p in the valence band is less than 20% of that corresponding to O 2s ($\sigma_{O2p^6}/\sigma_{O2s^2} = 0.19$ for Al Kα radiation). This evidences that the major part of the XP valence band spectrum is due to the photoemission of Mo 4d electrons. In order to obtain a more quantitative estimate for the total number n_d of Mo 4d electrons in occupied molecular orbitals we measured the valence band spectra of **4** and molybdenum metal relative to the respective peaks corresponding to Mo 4p electrons. The intensity ratios I_{4p}/I_{VB} are 2.36 for **4** and 2.49 for metallic molybdenum. Taking equal photoionization cross sections in molybdenum and **4**, $n_d(\mathbf{4})$ is estimated according to

$$n_d(\mathbf{4}) = n_d(Mo)f\frac{(I_{4p}/I_{VB})[\mathrm{Mo}]}{(I_{4p}/I_{VB})[\mathbf{4}]} \qquad (1)$$

It is assumed that the valence band spectrum of molybdenum is entirely due to photoemission from 4d orbitals as the photoemission cross section for 5s electrons is small. The factor

$$f = 1 - \frac{I_{O2p}}{I_{VB}} \approx 1 - \frac{\sigma_{O2p^6}I_{O2s}}{\sigma_{O2s^2}I_{VB}} \qquad (2)$$

takes into account the O 2p contribution to the valence band spectrum of **4**. With a $4d^55s^1$ configuration for molybdenum and the above intensity ratios one obtains an average number of 4.4 Mo 4d electrons per molybdenum center in **4**. This analysis demonstrates that the electronic structure and chemical bonding of the cluster compound are characterized as expected by strong covalent interactions between Mo 4d and O 2p orbitals as is also seen from the overlap of the Al Kα and He II valence band spectra (Figure 4). Whereas the Al Kα spectrum is dominated by the Mo 4d partial density of states, the He II spectrum mainly reflects the O 2p partial density of states. Pronounced covalent interactions between transition metal d orbitals and O 2p orbitals, leading to a strong deviation of the actual charge at the metal site from the formal oxidation state, are a general feature of the electronic structure of oxides with transition metal centers having high oxidation numbers (cf. the cases of manganese(VII)[14] and copper(III)[15]).

The most obvious difference in the Al Kα valence band spectra of **4** and **5** is the significantly increased photoemission observed at energies above the main band for the latter (Figure 4). Such a band is also seen in the He II spectrum of **5** but its relative intensity contribution is larger in the Al Kα spectrum. It is concluded that the additional electrons arising from the molybdenum(V) centers enter molecular orbitals of predominantly Mo 4d character. A small band corresponding to low binding energy is also seen in the XP valence band spectrum of **4**. Its nature is not completely clear, but it may correspond to a certain amount of molybdenum(V) created under UHV conditions and irradiation with X-rays.[16]

Widths and shapes of the peaks observed in the XP valence band spectra of **1b**, **2**, and **3** (Figure 5), where most of the molybdenum centers are in the formal +6 oxidation state, are very similar to those of **4**. In all three cases, **1b**, **2**, and **3**, in addition to the main band also a second band with small intensity at lower binding energies is found. It seems reasonable to assign these bands to the highest occupied levels arising from the $(MoNO)^{3+}$ orbitals in **3** as well as from the additional M(3d)−

(13) Yeh, J. J.; Lindau, I. *At. Data Nucl. Data Tables* **1985**, *32*, 1.

(14) Reinert, F.; Kumar, S.; Steiner, P.; Claessen, R.; Hüfner, S. *Z. Phys. B* **1994**, *94*, 431.

(15) Karlsson, K.; Gunnarsson, O.; Jepsen, O. *J. Phys. Condens. Matter* **1992**, *4*, 895.

(16) A partial reduction of molybdenum(VI) to molybdenum(V) may also be the reason for the rather large line width and asymmetry of the Mo 3d spectrum of **4**.

O(2p) (M = Fe, V) and Mo^{V}(4d)−O(2p) antibonding levels in **1b** and **2** (see below). But again, one must be aware of the possibility of a reduction of molybdenum(VI) sites during the rather long measuring times (about 15 h) required for a reasonable signal-to-noise ratio with the present equipment. In the case of **1b** the time dependence of the valence band spectra was investigated in more detail. In fact a certain increase in intensity of the band at low binding energy and a concomitant pronounced broadening of the Mo 3d lines is observed after long measuring times. But even a valence band spectrum collected within 1 h, a time where no changes in the signal corresponding to Mo 3d were observed, indicated already the presence of a band with low intensity above the main part of the valence band. Also the He II spectra of **1b** reveal such a band.[17] The fraction of the various sites is too low to allow a more detailed investigation of its nature. For this purpose resonant photoemission studies with excitation energies at the transition metal *n*p−*n*d threshold could be helpful.

Magnetic Properties. The treatment of the raw magnetic data of **1a**, **1b**, and **2** encounters some difficulties, because there are only a few magnetic centers embedded in giant cluster anions with a molecular weight larger than 9 kDa. Furthermore, the large number of molybdenum(VI) centers in these moieties results in a nonnegligible temperature independent paramagnetic (TIP) contribution.[18] In order to tackle these problems we used **3** as a standard to estimate the diamagnetic and TIP contributions to the overall molecular susceptibility of **1a**, **1b**, and **2**. This is possible since the cluster anion of **3** contains two of the Mo_{17} ligands also composing **1a**, **1b**, and **2**, which are linked by diamagnetic $(MoO_2)^{2+}$ centers. Therefore we measured the susceptibility of **3**, which has a molecular weight of 6401 Da, and found a susceptibility of -1×10^{-3} emu mol^{-1}, practically independent of temperature. Compared to the diamagnetic susceptibility expected according to Pascal's corrections the measured value for compound **3** clearly shows the presence of a rather large TIP contribution. The measured susceptibility of **3**, scaled for the ratio of the molecular weights **1a**/**3**, **1b**/**3**, and **2**/**3**, respectively, was used to calculate the susceptibilities of **1a**, **1b**, and **2**, corrected for diamagnetic contributions, shown in Figure 6.

The room temperature value of χT for the iron(III) compound **2** (27.7 emu mol^{-1} K) corresponds well with the value expected for six uncoupled iron(III) centers (26.25 emu mol^{-1} K), showing that the correction we used is meaningful. The corresponding χT value for **1a** (1.2 emu mol^{-1} K) is much smaller than expected for six uncoupled $S = {}^1/_2$ spins (2.25 emu mol^{-1} K) indicating strong antiferromagnetic coupling.[19] For **2** the χT value (see Figure 6a) decreases slowly on decreasing the temperature down to ca. 80 K, and below this temperature much more rapidly, reaching 4.6 emu mol^{-1} K at 2.5 K. The susceptibility seems to go through a maximum in this range of temperature.

The χT behavior observed for **1a** (see Figure 6b) is quite different, decreasing smoothly down to 80 K. Between this temperature and ca. 40 K it is substantially constant at ca. 0.7 emu mol^{-1} K, the value expected for two uncoupled $S = {}^1/_2$ spins. Below 30 K χT decreases rapidly, reaching 0.5 emu mol^{-1} K at 2.3 K. A similar behavior is obtained for **1b** (see Figure 6c), except that the leveling of χT occurs at the value of 0.65 emu mol^{-1} K, and the further decrease starts at ca. 50 K to reach the value of 0.43 emu mol^{-1} K at 2.3 K.

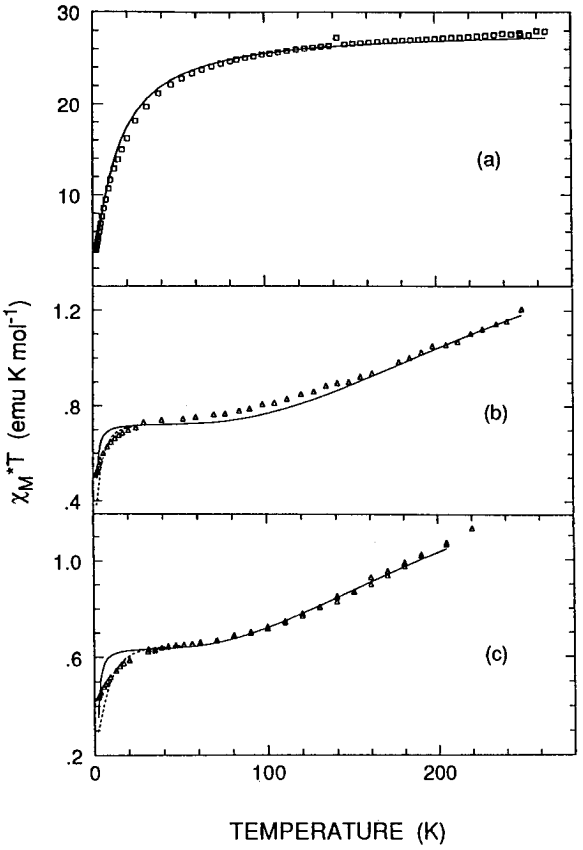

Figure 6. Temperature dependence of the product of the magnetic susceptibility with temperature for **2** (a), **1a** (b), and **1b** (c). The solid lines represent the calculated values using a two-J model (see text) with the following parameters: $g = 2.05$, $J = 1.2$ cm^{-1}, and $J' = 0.05$ cm^{-1} for **2**, $g = 1.97$, $J = 195$ cm^{-1}, and $J' = 2.6$ cm^{-1} for **1a**, and $g = 1.85$, $J = 158$ cm^{-1}, and $J' = 3.3$ cm^{-1} for **1b**. The dashed lines in parts b and c are the calculated values, taking into account the antisymmetric exchange (see text).

In the cluster anions of **1a**, **1b**, and **2** there are several magnetic centers: six molybdenum(V) and six vanadium(IV) (iron(III)), assuming that the NO groups are covalently bound to their molybdenum centers yielding diamagnetic groups (see Figure 7). The molybdenum(V) centers are linked in pairs to each other, the $\{Mo(\mu\text{-}H_2O)_2(\mu\text{-}OH)Mo\}^{9+}$ moieties, with relatively short metal−metal distances, forming bridges between the Mo_{17} ligands. The comparison with simple comparable compounds suggests that all these pairs are diamagnetic,[5,20] due to extremely strong antiferromagnetic exchange interactions. In fact, this view is confirmed by the room temperature magnetic data for **2**, which corresponds to six very weakly coupled iron(III) centers. We can therefore safely assume that the magnetic properties of the two giant cluster anions must be dominated by the **M** centers (iron, vanadium; cf. Figure 2).

The arrangement of the magnetic centers **M** is very interesting, because it corresponds to two equilateral triangles. It is well known that in the presence of antiferromagnetic interactions such an arrangement gives rise to spin frustration effects.[21] The spin ground states for the individual triangles, composed of three

(17) The detailed shapes of the He II spectra of the compounds should be treated with some caution as the spectra are sensitive to the parameters of the flood gun. Therefore these spectra will not be compared further in this work.

(18) Carlin, R. L. *Magnetochemistry*; Springer Verlag: New York, 1986.

(19) This result is consistent with the fact that the ESR spectra reported earlier for compounds **1a** and **1b** (cf. ref 7 and Müller and Plass: Müller, A.; Plass, W. *J. Mol. Struct.* **1994**, *321*, 215) turned out to be due to an impurity owing to the preparation procedure.

(20) Müller, A.; Krickemeyer, E.; Penk, M.; Wittneben, V.; Döring, J. *Angew. Chem., Int. Ed. Engl.* **1990**, *29*, 88.

(21) Vannimenus, J.; Toulouse, G. *J. Phys. C: Solid State Phys.* **1977**, *10*, L537.

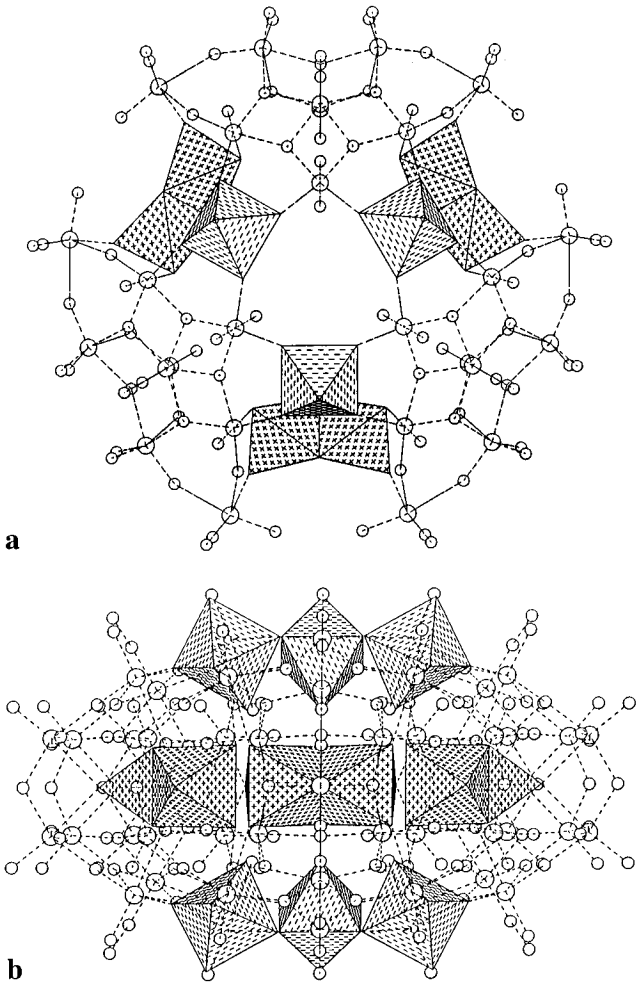

Figure 7. Demonstration of the open shell 3d centers of the cluster anions of **1a** (**1b**) and **2** (for metal-metal distances see text): (a) view approximately along and (b) view perpendicular to the $\bar{6}$ (S_3) axis.

$S = {}^1/_2$ or three $S = {}^5/_2$ interacting spins, are expected to be two degenerate $S = {}^1/_2$ states, in the limit of only isotropic exchange present, which can be referred to as ^{2}E.[22] In this notation it is clear that there is some form of orbital degeneracy in the ground state of the frustrated triangle, and therefore the system must be unstable towards perturbations which remove the degeneracy. For isolated triangles this can be brought about by spin−orbit coupling, which gives rise to antisymmetric exchange, or by phonon coupling which lowers the symmetry of the clusters.

We tried to fit the magnetic data using isotropic exchange and the two parameters, J for the coupling within the triangles and J' for the coupling between the triangles:

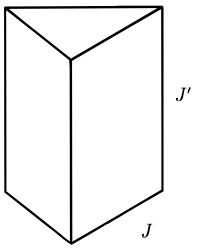

The best fit curve obtained for **2** with $g = 2.05$, $J = 1.2$ cm^{-1}, and $J' = 0.05$ cm^{-1} is shown in Figure 6a. The fit can be considered as very satisfactorily. Actually only the value of J can be meaningfully obtained, while J' remains substantially undefined, because it is expected to give sizable effects only below 4 K. The small value of J is not unexpected for two d^5 ions which are rather far apart from each other.[23]

The situation is different in the case of **1a** and even more so for **1b**, where the two-parameter fit is not satisfactory. There is no doubt, as seen for the experimental data, that a strong antiferromagnetic coupling operates within the two triangles, with J of ca. 190 cm^{-1} from **1a** and ca. 160 cm^{-1} for **1b**. Compared with the corresponding value for the iron derivative, and for the constants usually observed in oxovanadium(IV) clusters, this value is abnormally high.[24,25] In fact J values of ca. 20 cm^{-1} were reported for O−As−O bridges.[25] Further, the inclusion of J' is not sufficient to really fit the low temperature data, as shown in Figure 6b,c where the solid lines represent the calculated values with the best fit parameters: $g = 1.97$, $J = 195$ cm^{-1}, and $J' = 2.6$ cm^{-1} for **1a** and $g = 1.85$, $J = 158$ cm^{-1}, and $J' = 3.3$ cm^{-1} for **1b**. In particular, for **1b**, it is apparent that the experimental χT does not tend to zero at 0 K, which is not in agreement with the diamagnetic ground state predicted by this model. Assuming that the inter-triangle exchange interaction is negligible also in the case of V(IV) spins we can consider the effects of the antisymmetric exchange in the three spin system. The Hamiltonian takes the form

$$\hat{H} = \sum_{ij} \mathbf{G}_{ij}[\mathbf{S}_i \times \mathbf{S}_j] \tag{3}$$

where $\mathbf{G}_{ij}$ is a vector, which usually is taken as a parameter. Its physical origin is the admixture of excited states into the ground state through spin−orbit coupling. To the second order in perturbation theory it is given by[26,27]

$$\mathbf{G}_{ij} = \mathbf{G}_i - \mathbf{G}_j \tag{4}$$

with

$$\mathbf{G}_i = 2\sum_n \Delta_n^{-1} \lambda_n \langle n_i|\mathbf{L}_i|g_i\rangle\langle n_i g_i|\hat{H}_{ex}|g_i g_j\rangle \tag{5}$$

where the sum is over all excited states $|n_i\rangle$, separated by an energy Δ_n from the ground state $|g_i\rangle$, λ_n is the spin−orbit coupling constant and $\hat{H}_{ex}$ is the electron exchange Hamiltonian. For a triangular cluster the only relevant component of $\mathbf{G}_{ij}$ is the one parallel to the trigonal axis, characterized by a parameter G_{ij}. Often the G_{ij} parameter is estimated on an order of magnitude basis as[27]

$$G_{ij} \approx \Delta g/gJ \tag{6}$$

where Δg is the deviation of the average g value of the coupled centers from $g_e = 2.0023$, and J is the isotropic coupling constant. For the present case an estimate of G_{ij} gives ca. 7 cm^{-1}.

(22) Tsukerblatt, B. S.; Belinskii, M. I.; Fainzil'berg, V. E. *Sov. Sci. Rev. B: Chem.* (*Engl. Transl.*) **1987**, *9*, 339.

(23) Gorun, S. M.; Lippard, S. J. *Inorg. Chem.* **1991**, *30*, 1625.

(24) (a) Gatteschi, D.; Pardi, L.; Barra, A.-L.; Müller, A. *Mol. Eng.* **1993**, *3*, 157. (b) Gatteschi, D.; Pardi, L.; Barra, A.-L.; Müller, A.; Döring, J. *Nature* **1991**, *354*, 463. (c) Barra, A.-L.; Gatteschi, D.; Tsukerblatt, B. S.; Döring, J.; Müller, A.; Brunel, L.-C. *Inorg. Chem.* **1992**, *31*, 5132. (d) Gatteschi, D.; Tsukerblatt, B. S.; Barra, A.-L.; Brunel, L.-C.; Müller, A.; Döring, J. *Inorg. Chem.* **1993**, *32*, 2114. (e) Müller, A.; Rohlfing, R.; Barra, A.-L.; Gatteschi, D. *Adv. Mater.* **1993**, *5*, 915.

(25) Barra, A.-L.; Gatteschi, D.; Pardi, L.; Müller, A.; Döring, J. *J. Am. Chem. Soc.* **1992**, *114*, 8509.

(26) Dzyaloshinsky, I. *J. Phys. Chem. Solids* **1958**, *4*, 241.

(27) Moriya, T. *Phys. Rev.* **1960**, *117*, 635.

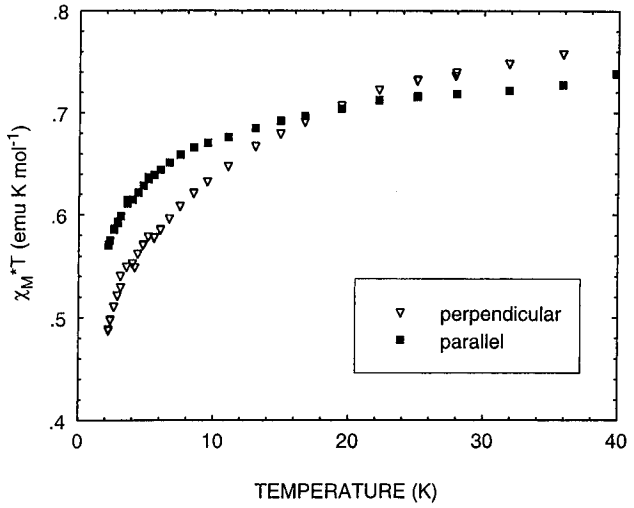

Figure 8. Temperature dependence of the χT product for **1a** observed by applying the field parallel and perpendicular to the unique *c* axis.

The result of applying the Hamiltonian 3 to a trimer of spin $S = {}^1/_2$ is that of splitting ^{2}E into two Kramers doublets separated by $3\sqrt{3}G_{ij}$. This splitting has large effects on the magnetic susceptibility of the trinuclear clusters, and in particular on the magnetic anisotropy. In fact, the parallel susceptibility is substantially unaffected, while the perpendicular susceptibility is strongly affected at low field and low temperatures. It is given by[22]

$$\chi_{\perp} = N(g\mu_B)^2 \frac{\tanh\left(\frac{\sqrt{4G^2 + (g\mu_B H)^2}}{2kT}\right)}{\sqrt{4G^2 + (g\mu_B H)^2}} \qquad (7)$$

where $G = 3G_{ij}$ and H is the applied magnetic field. At high temperature and high field $\chi_{\perp}$ goes to the limit $\chi_{\perp} = {}^3/_4\,(N_{g\perp}\mu_B{}^2)/(3kT)$, which differs from the corresponding expression for $\chi_{\parallel}$ only for the value of g ($g_{\perp}$ instead of $g_{\parallel}$). However, at low temperature where $G > kT$ $\chi_{\perp}$ is expected to decrease rapidly, thus giving rise to a temperature dependent magnetic anisotropy. This theoretical prediction finds a nice confirmation in the experimental magnetic anisotropy measurement shown in Figure 8. Above 20 K the susceptibility is larger when measured in the *ab* plane as expected with $g_{\perp} > g_{\parallel}$ for VO^{2+} centers. Below this temperature the anisotropy changes sign and increases with decreasing temperature. This effect cannot be due to *g* anisotropy, since in this case it would be temperature independent.

We fitted the low temperature powder susceptibility of **1a** and **1b** using eq 7 and the best fit is shown in parts b and c of Figure 6, respectively, as dashed lines. It can be considered as satisfactory and definitely better than that obtained with the two-*J* model, especially for **1b**. The values of *G*, 5 and 9 cm^{-1}, found for **1a** and **1b** respectively, are in agreement with the order-of-magnitude estimate made on the basis of eq 6.

From Figure 8 it is apparent that a decrease in χT also occurs when the field is parallel to the unique axis. This can be due either to partial misalignment of the crystal or to the presence of antiferromagnetic interactions between the triangles.

Although the necessity to introduce antisymmetric exchange in the treatment of the magnetic data of highly symmetric spin clusters has long been known, to our knowledge this is the first time that magnetic anisotropy measurements can be employed to unambiguously proof it.

The other unusual feature of the magnetization of **1a** and **1b** is the strong antiferromagnetic coupling between oxovanadium(IV) centers which are more than 600 pm apart. In order to elaborate a semiquantitative model we performed extended Hückel MO calculations.

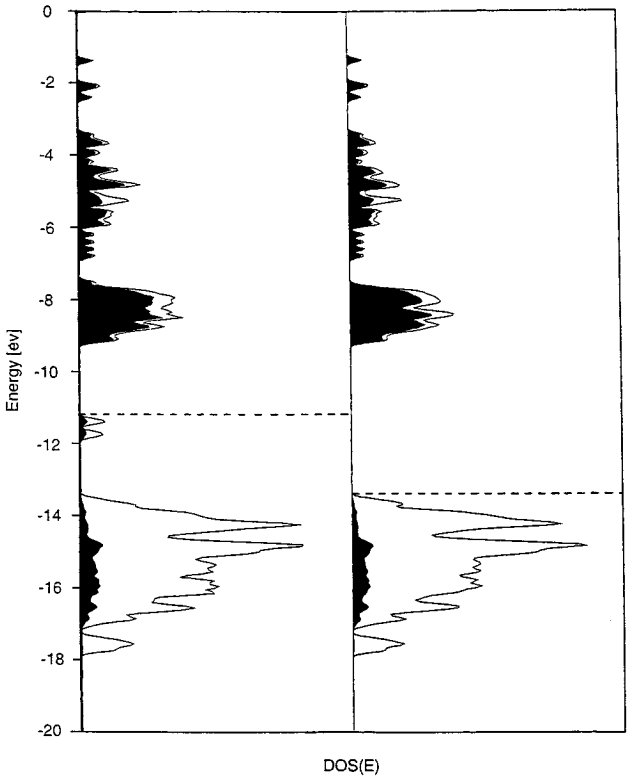

Figure 9. Representation of the density of states (DOS) diagrams of the cluster anions of compounds **3** (on the left) and **4** (on the right). The contributions of the Mo 4d orbitals to the total DOS are represented by the solid areas in the diagrams.

Extended Hückel Calculations. Extended Hückel MO calculations[28] were performed on the cluster anions of compounds **1a** (**1b**), **2**, **3**, **4**, and **5** in order to derive a qualitative picture of the electronic structure of such large metal oxide assemblies and to possibly elucidate why polyoxometalate fragments, like the Mo_{17} ligands, are mediating the exchange interactions between paramagnetic metal centers so efficiently.

As expected for compounds with metal centers in *high* oxidation states, like the polyoxometalates and in agreement with the results from photoelectron spectroscopy, the electronic structure can be related to that obtained for a corresponding single metal oxygen fragment MoO_x. This can be shown by model calculations on a series of cluster anions with an increasing number of metal centers. Typically a clear separation is observed between the Mo(4d)−O(2p) antibonding levels (LUMO) and the levels composed predominantly of O 2p orbitals with metal oxygen bonding character (HOMO). Upon increasing the number of metal centers the density of states increases in the HOMO and LUMO region. This can, for instance, easily be visualized by comparing the MO schemes of the anions $[MoO_4]^{2-}$ and $[PMo_{12}O_{40}]^{3-}$ (for a comparable study on MoO_x see ref 33). In the case of the polyoxomolybdates **3** and **4** we can already consider the two aforementioned

(28) For the cluster anions of compounds **3**, **4**, and **5** we also performed SCCC type calculations,[29] using a modified version[30] of the EHT-SPD program.[31] The basis sets and H_{ii}'s were taken from ref 32 and the geometrical data from published structure determinations.[6,7]

(29) Basch, H.; Viste, A.; Gray, H. B. *Theor. Chim. Acta* **1965**, *3*, 458.
(30) Jostes, R. Ph.D. Thesis, University of Bielefeld, 1984.
(31) Diboult, P. EHT-SPD. *QCPE* **1976**, No. 256.
(32) Clementi, E.; Roetti, C. *At. Data Nucl. Data Tables* **1974**, *14*, 177.
(33) Jansen, S. A.; Singh, D. J.; Wang, S.-H. *Chem. Mater.* **1994**, *6*, 146.

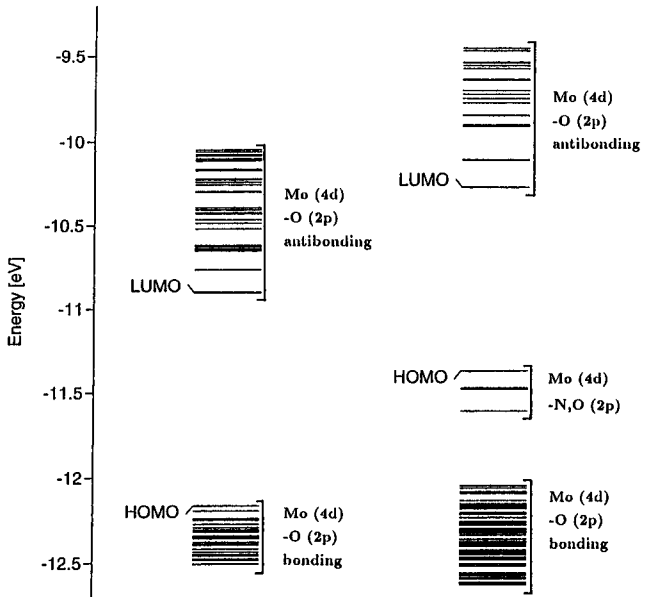

Figure 10. Representation of the MO schemes in the HOMO−LUMO region of the cluster anions of compounds **3** (on the right) and **4** (on the left).

groups of orbitals as quasi-bands (see Figure 9), and upon going to the cluster anions of **1a** (**1b**) and **2** this effect is even more pronounced. The ionization of electrons from the quasi-band composed of the O(2p)-Mo(4d) bonding levels constitutes the main part of the valence band photoelectron spectra of all compounds investigated herein.

The anion of **3** can formally be derived from that of **4** by replacing four $(MoO)^{4+}$ groups by $(MoNO)^{3+}$ units. Therefore, a third group of eight orbitals with Mo−NO character is located in the HOMO−LUMO region of **3**, with the highest energy orbital of these representing the HOMO. The MO schemes obtained for the cluster anions of **3** and **4** utilizing SCCC−EHMO calculations[28] are represented in Figure 10. Due to the charge iteration procedure in the SCCC−EHMO calculations the HOMO−LUMO energy gaps become smaller and the energy levels of the higher negatively charged cluster anion of **3** shift to higher energies, but the qualitative picture derived from the EHMO calculations (see Figure 9) is retained. A Mulliken population analysis for the cluster anion of **3** reveals relatively large contributions of the corresponding Mo 4d orbitals to the MOs with Mo−NO character (see also Figure 9) and is, therefore, in agreement with the observation of a small band in the XP valence band spectrum of **3** at lower binding energy and also with the smaller Mo 3d core level binding energy for the Mo atoms from the $(MoNO)^{3+}$ groups (see section on Photoelectron Spectroscopy).

The situation is different when cluster anions with partially reduced molybdenum centers are considered. The DOS diagram of the cluster anion of compound **5** is depicted in Figure 11. In this cluster anion Mo(4d)−O(2p) antibonding levels get occupied and, therefore, a relatively small HOMO−LUMO energy separation is observed. This is consistent with the observation of a less intense band at lower binding energy, mainly of Mo 4d character, in the valence band region of the photoelectron spectra of **5** (see also Figure 4).

For the cluster anions of compounds **1a** (**1b**) and **2** we have to expect both of the above discussed contributions to the HOMO−LUMO region, the MOs with Mo−NO character from the six $(MoNO)^{3+}$ groups as well as populated Mo(4d)−O(2p) antibonding levels due to the additional Mo 4d electrons of the cationic $\{Mo(\mu\text{-}H_2O)_2(\mu\text{-}OH)Mo\}^{9+}$ moieties. A third contribution to the HOMO−LUMO region arises from the metal centers with occupied V 3d and Fe 3d levels, respectively. The contributions from the additional M(3d)−O(2p) (M = Fe, V) and Mo^{V}(4d)−O(2p) antibonding levels as well as the $(MoNO)^{3+}$ orbitals to the HOMO region are consistent with the observation of a small band at low binding energy in the photoelectron spectra of **1b** and **2**, especially if the time dependence of the valence band spectra of **1b** is considered, which indicates the intrinsic character of this feature. Unfortunately, photoelectron spectroscopy does not provide any distinct information about the three aforementioned contributions to the HOMO−LUMO region of these cluster anions.

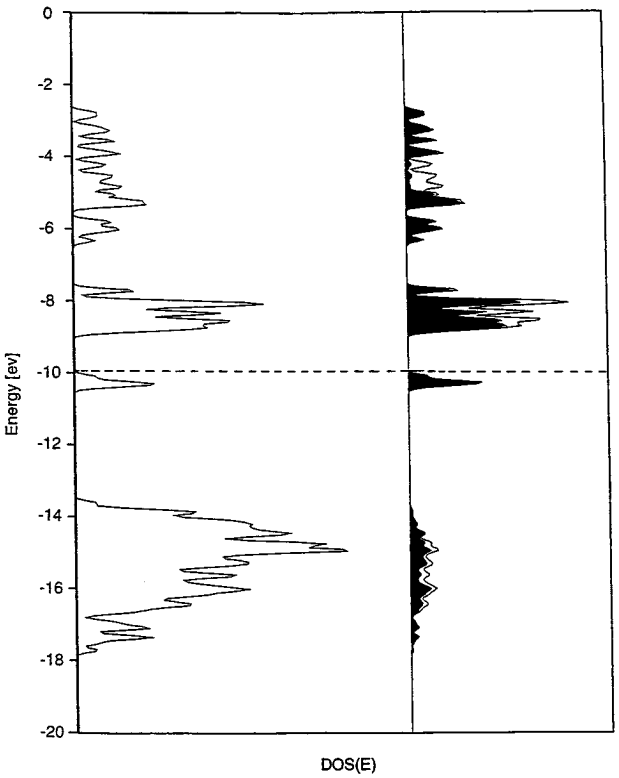

Figure 11. Representation of the density of states (DOS) diagram of the cluster anion of compound **5** (on the left). The contributions of all Mo 4d orbitals to the DOS (at the same scale) are depicted on the right, with the contributions of the twelve Mo(V) centers emphasized in black.

EHMO calculations on the cluster anions of compounds **1a** (**1b**) and **2** are consistent with the qualitative picture outlined above. As in the case of compound **3**, the MOs with the Mo−NO character from the $(MoNO)^{3+}$ groups are located above the Mo(4d)−O(2p) bonding levels. However, no clear energetic separation is found between orbitals with predominant M 3d (Fe or V) and Mo 4d character. As a consequence we cannot unambiguously assign the character of the HOMO in these cluster anions. Moreover, the situation is complicated by the fact that there are no antibonding Mo(4d)−O(2p) levels solely constituted by contributions from the Mo(V) centers, i.e. there are no antibonding levels with predominant Mo(V) contributions. Due to this fact we did not succeed in performing a SCCC−EHMO calculation converging to a reasonable charge distribution, which clearly demonstrates the limitations of the EHMO methodology (electron−electron interactions can be expected to be rather important for such an open shell case).

However, we can still draw some qualitative conclusions from the EHMO calculations on the anions of compounds **1a** (**1b**) and **2**. The calculations clearly demonstrate that polyoxometalate ligands suit extremely well the energetic requirements for the interaction with open shell metal centers such as V(IV) and

Fe(III). From the fact that Fe 3d levels are generally lower in energy than the V 3d ones (H_{ii}'s: Fe 12.60, V 11.18, Mo 10.50 eV) one may expect a more pronounced energetic separation of the levels within the HOMO region for the vanadium case, i.e. between the Mo(4d)−O(2p) bonding levels and M(3d)−O(2p) (M = Fe, V) antibonding levels. This would be consistent with small differences in the XP valence band spectra of **1b** and **2**, indicating a smaller mean separation of the bands constituting the HOMO region (Figure 5) from the main band for the latter.

Why can the Mo_{17} ligand be such an efficient mediator for exchange interactions between paramagnetic metal centers? The MO scheme depicted in Figure 10 represents qualitatively that of two superimposed independent Mo_{17} moieties, the HOMO−LUMO region of which fits energetically quite well to metal 3d levels. Along with the high density of states in the LUMO region, it is this energetic tuning that enables such efficient exchange pathways.

Conclusions

1a, **1b**, and **2** are examples of inorganic systems which resemble formally metalloproteins. The diamagnetic Mo_{17} ligands have the role of the apoprotein fragments which define the location of the "active site" M_6. However, these Mo_{17} moieties have not only a structural function, but participate actively in determining the function of the $\mathbf{M}_6$ clusters; i.e., they transmit the magnetic interaction between them. It is certainly a remarkable result that they are so effective in transmitting the interaction between vanadium(IV) centers. One important fact in this respect is definitely the high density of states in the LUMO region of the resulting giant cluster anions. This finding opens new perspectives for the magnetic properties of large clusters especially heteropolyoxomolybdates.

The insulation of the V_6 centers in the active site of **1a** and **1b** allowed a detailed investigation of the magnetic properties of these compounds without having to worry about intermolecular interactions. In fact the shortest intermolecular V−V distances are 800 pm. This allowed us to determine for the first time with some accuracy the elusive antisymmetric exchange parameter *G*. This is expected to be operative in all spin-frustrated systems, but has been largely neglected up to now. Given the relevance of spin-frustrated systems in many biologically interesting compounds, it is of fundamental importance that experimental confirmation of its presence is finally achieved.

Acknowledgment. We thank the Deutsche Forschungsgemeinschaft, the Fonds der Chemischen Industrie, the MURST, and the Council of the European Community (Grant ERB-CHRXCT920080) for the financial support. We are grateful to W. Hölle for measuring the photoelectron spectra.

IC951085L